A model for drop and bubble breakup frequency based on turbulence spectra

Benjamin Lalanne, Olivier Masbernat, Frédéric Risso

A Model for Drop and Bubble Breakup Frequency Based on Turbulence Spectra

Benjamin Lalanne* and **Olivier Masbernat**
Laboratoire de Génie Chimique (LGC), Université de Toulouse, CNRS, Toulouse, France and FERMAT, Université de Toulouse, CNRS, INPT, INSA, UPS, Toulouse, France

Frédéric Risso
Institut de Mécanique des Fluides de Toulouse (IMFT), Université de Toulouse, CNRS, Toulouse, France and FERMAT, Université de Toulouse, CNRS, INPT, INSA, UPS, Toulouse, France

DOI 10.1002/aic.16374
Published online in Wiley Online Library (wileyonlinelibrary.com)

In this article, a new Eulerian model for breakup frequency of drops induced by inertial stress in homogeneous isotropic turbulence is developed for moderately viscous fluids, accounting for the finite response time of drops to deform. The dynamics of drop shape in a turbulent flow is described by a linear damped oscillator forced by the instantaneous turbulent fluctuations at the drop scale. The criterion for breakup is based on a maximum value of drop deformation, in contrast with the usual critical Weber criterion. The breakup frequency is then modeled as a function of the power spectrum of Weber number (or velocity square), based on the theory of oscillators forced by a random signal, which can be related to classical statistical quantities, such as dissipation rate and velocity variance. Moreover, the effect of viscosities of both phases is included in the breakup frequency model without resorting to any additional parameter. © 2018 American Institute of Chemical Engineers *AIChE J*, 00: 000 000, 2018

Keywords: drops and bubbles, breakup frequency, breakup kernel, forced oscillator, turbulent flow, stochastic process

Introduction

In chemical processes involving flows with drops or bubbles, the control of interfacial area is a key issue for heat and mass transfer rates, transport properties of mixtures, and phase separation problems. Examples include two phase flows in stirred tanks, bubble column reactors, pipes, emulsification processes, where the flow regime is generally turbulent. In the modeling of such processes involving dispersed phases, computational fluid dynamics (CFD) tools are frequently used in combination with population balance equations to predict drop or bubble size distribution. These equations include modeling of breakup and coalescence rates, by means of closure terms.

The choice of a breakup closure model depends on the nature of the mechanism responsible for breakup. We consider here breakup of preexisting drops or bubbles that are traveling in a continuous phase, which is often referred to as secondary breakup (by opposition to primary breakup which refers to the initial formation of an emulsion from two merging flows). Under these conditions, breakup of drops or bubbles can be induced by different stresses: (i) turbulent pressure fluctuations in the continuous phase that deform drop which size lies in the inertial range of turbulence, (ii) viscous shear forces resulting from velocity gradients around the drop, which can originate from either laminar shear or turbulent shear if the drop is smaller than the Kolmogorov scale, (iii) inertial forces due to a strong drift velocity between the drop and the continuous phase or in case of a strong acceleration/deceleration in the flow. Besides, several stresses resist to drop deformation: a surface stress due to the interfacial tension, and an internal viscous stress when viscosity of the dispersed phase is high. In a given flow, different breakup mechanisms have to be evaluated by calculating the Weber or capillary numbers based on the various sources of stress at the scale of the drop. In this article, we only address the case (i) of inertial turbulent breakup, where the dominant contribution for drop deformation is a turbulent forcing (i.e., dynamic pressure fluctuations at the drop scale), and where resistance to deformation is predominantly controlled by the interfacial tension and not by the inner phase viscosity (limit of small Ohnesorge number).

In the literature, a lot of models for the breakup frequency have been developed; the papers of Lasheras et al.[1] (in the case of breakup in a turbulent flow), Liao and Lucas,[2] and Solsvik et al.[3] review and compare them. It is shown that these models can give very different results with several orders of magnitude of discrepancy on the breakup frequency, and that some of them contain several adjustable parameters or a choice for limits in integral calculations that have a huge influence on the model predictions. Even the evolution of the breakup frequency with the drop diameter is under discussion, several models predicting a strictly monotonous functions whereas other ones exhibit a maximum. Validation of these models by experimental data is still problematic, as these quantities are often space and time averaged in non homogeneous turbulent flows (pipe flows, stirred tanks, static

mixers, etc.). In addition, the collection of statistically converged breakup probability or frequency in such experimental devices is a hard task to achieve, in particular due to low probability of highest pressure fluctuations and to limited residence time of drops or bubbles in the flow area of interest. As a result, experimental data may exibit opposite trends, making difficult their interpretation with statistical models. In view of assessing breakup frequency models in turbulent flows, it is therefore necessary to develop numerical and physical breakup experiments which fully verify the statistical convergence in space and time of the deformation process.

Following the pioneering work of Kolmogorov[4] and Hinze,[5] most of the existing models consider the turbulent flow like a discrete array of eddies at the scale of drop or bubble size, and they assume that a breakup event occurs when the kinetic energy of a turbulent eddy is sufficient to overcome surface tension, that is, they suppose the existence of a critical Weber number for breakup. Some breakup frequency expressions are obtained directly from a modeling of the probability density function of the turbulent kinetic energy of the eddies[6-9] (using different statistical laws: normal law, Maxwell's law, etc.). Other models multiply a collision frequency between eddies and drops with a collision efficiency.[10-12] In the case of air bubbles in a liquid jet, further extended by Eastwood et al.[13] for liquid–liquid systems, Martinez-Bazan et al.[14] consider that the characteristic velocity of the breakup process is proportional to the difference between the dynamic pressure produced by the turbulent fluctuations at the drop scale and the restoring pressure force induced by interfacial tension, leading to a breakup frequency proportional to the square root of the Weber number.

One common idea to these models is the existence of a critical Weber number for breakup, resulting from a force balance between turbulent pressure force and surface tension force. If such a critical value exists, it is not universal. As shown by Risso,[15] this static balance is not suitable in cases where the residence time of the drop or bubble is large compare to the period of shape oscillation of the drops, as discussed in the present article. A few other works insist on the importance of the dynamic response of the drop, like the study of Sevik and Park,[16] who postulate a resonance mechanism between the bubble dynamics and turbulent fluctuations, or the work of Zhao and Ge[17] who introduce the concept of eddy efficiency by considering that the time scale of response of the drops to turbulent fluctuations controls the maximal amount of energy that can be extracted from each turbulent eddy. The importance of the resonance mechanism between turbulent fluctuations and bubble dynamics in the breakup problem has been shown in detail in the paper of Risso and Fabre,[18] and a model for the breakup probability was proposed. This model has been successfully compared to experimental data on breakup statistics in non homogeneous turbulent flows in the case of liquid–liquid dispersions, from dilute up to concentrated emulsions at 20 vol %.[19,20] In the context of atomization, note that a similar dynamic model exists for the calculation of low Weber number engineering sprays, known as the Taylor analogy breakup model,[21] which accounts for the coupling between interface dynamics and aerodynamic forces responsible for breakup due to the relative velocity between the drops and the gas phase in that case.

First, the physical basis and range of validity of the Lagrangian model proposed by Risso and Fabre[18] is discussed, both from elementary examples and from comparison of new experimental data of breakup in a liquid–liquid system. One major interest of this approach is to account for the finite time of a breakup event. Another interesting feature of this dynamic model is to include the contribution of densities and viscosities of both phases in an explicit way, in the limit of low Ohnesorge number of the dispersed phase (resistance to drop deformation is controlled by surface tension).

Then, by combining computations of this Lagrangian model with experimental measurements of turbulent fluctuations in an isotropic turbulent flow, statistics on the breakup frequency are collected, and a new breakup frequency law is derived based on turbulence spectra properties. Finally, scalings of these statistical quantities valid in the inertial range of turbulence are introduced into this Eulerian law of breakup frequency, with the objective to implement this model in population balance codes for industrial applications, in future works.

A Dynamic Model for Drop Deformation

Force and time scales of interface and flow

We consider a drop or a bubble of diameter d, of density and dynamic viscosity ρ_d and μ_d, respectively, immersed in a carrier fluid of density and dynamic viscosity ρ_c and μ_c, respectively. The interfacial tension between the two phases is denoted σ and is assumed to be constant: no dynamic effects due to a possible presence of surfactants adsorbed at the interface are considered here. In the following, the fluid particle will be called a drop, but it can be a bubble as well.

Interface Dynamics. Surface tension induces an interfacial stress $F_s \propto \frac{\sigma}{d}$ that maintains the drop shape so as to minimize surface energy. Then, when the shape of a drop is shortly disturbed whatever the cause of surface perturbation, it undergoes oscillations damped by viscous effects, until recovering its equilibrium shape. This problem has been addressed theoretically by several authors (Rayleigh,[22] Lamb,[23] Miller and Scriven,[24] Lu and Apfel,[25] Prosperetti[26]) in the case of low amplitude shape oscillations, its solution showing that the interface dynamics can be expressed as a series of eigenmodes. Each mode describes the dynamics of a particular shape, and is associated with both an eigenfrequency of oscillation and a damping rate. Mode 2 represents the oscillation between a prolate and an oblate drop shape. As it is the deformation mode of lowest energy (the mode with the lowest frequency), Mode 2 is the most easily excited and drop breakup is often observed to be associated with a prolate shape. Thus, Mode 2 gives a good description of the drop prevalent deformation; by denoting $A(t)$ the amplitude of this axisymmetric mode of deformation, the droplet shape deformed only along this mode can be written, in polar coordinates (r, θ), as $r(\theta,t) = R + A(t).\frac{1}{2}.(3\cos^2(\theta) - 1)$ with R the undeformed drop let radius. $A(t)$ is an oscillating signal at eigenfrequency ω_2 and damped at a rate β_2; these characteristics of Mode 2 thus define the timescales of the interface dynamics ($T_2 = 2\pi/\omega_2$ is the period of shape oscillation and $t_v = 1/\beta_2$ is the characteristic time of damping of the amplitude of oscillation).

ω_2 and β_2 can be obtained by solving numerically a general nonlinear equation given by Prosperetti (Eq. 33 in his paper of 1980). Note that these expressions explicitly account for the role of density and viscosity of both phases without the need of any empirical results; for a given size, values of ω_2 and β_2 are different in the cases of a drop or a bubble immersed in another liquid. In the limit of weak viscous effects (i.e., $\xi = \beta_2/\omega_2 \ll 1$), estimations of these time scales can be obtained from an asymptotic development,[24,25] which gives:

$$\begin{cases} \omega_2 \approx \omega_2^0 \left[1 - \dfrac{F}{\sqrt{Re_{OSC}}}\right] \\ \beta_2 \approx \dfrac{\omega_2^0}{Re_{OSC}} \{F\sqrt{Re_{OSC}} - 2F^2 + G\}, \end{cases} \quad (1)$$

where $\hat{\rho} = \rho_c/\rho_d$, $\hat{\mu} = \mu_c/\mu_d$, $F = \dfrac{25\,(\hat{\rho}\hat{\mu})^{1/2}}{2\sqrt{2\gamma}\left[1 + (\hat{\rho}\hat{\mu})^{1/2}\right]}$,

$G = \dfrac{5\left[6 + 4\hat{\mu} - \hat{\rho}\hat{\mu} + 16\hat{\rho}\hat{\mu}^2\right]}{2\gamma\left[1 + (\hat{\rho}\hat{\mu})^{1/2}\right]^2}$, $\gamma = 2\hat{\rho} + 3$,

$\omega_2^0 = \sqrt{\dfrac{\sigma}{d^3}\dfrac{192}{2\rho_c + 3\rho_d}}$ and $Re_{OSC} = \dfrac{\rho_d\,\omega_2^0\,d^2}{4\mu_d}$.

As examples, in the case of an air bubble in water, the deviation of Eq. 1 compared to a numerical solution of the (exact) nonlinear equation is <5% provided $Re_{OSC} \geq 5$ for ω_2 and provided $Re_{OSC} \geq 100$ for β_2. Then, in the case of an heptane drop in water, the same accuracy is reached for ω_2 when $Re_{OSC} \geq 30$, and for β_2 when $Re_{OSC} \geq 150$.

In the expressions given by Eq. 1, ω_2 and β_2 include a contribution from both the potential flow rising from the oscillating motion far from the interface, and the boundary layers that develop in each fluid close to the interface, the latter contribution corresponding to the terms proportional to $\sqrt{Re_{OSC}}$. Note that the contribution of the viscous boundary layers is negligible in the expression of ω_2, which is well predicted by the Lamb inviscid frequency ω_2^0, whereas it is a dominant term in the expression of β_2 in general. Indeed, frequency is mainly driven by inertial effects with a contribution of density of both dispersed and continuous phases, and surface tension, like in a spring mass system. At the opposite, damping rate β_2 is increasing with the viscosity of each phase.

Even if expressions of Eq. 1 have been obtained without considering the influence of gravity in the shape oscillations, they are generally still valid in the presence of a buoyancy induced motion, under the conditions given by Lalanne et al.[27,28] Moreover, more complex expressions of ω_2 and β_2 can also be computed by considering effect of surfactants[24,25,29] adsorbed at the drop surface.

Turbulent Flow. We consider now that the drop is traveling in a turbulent flow, and that the main cause of drop deformation and breakup is due to turbulent pressure fluctuations. The drop size is supposed to lie within the inertial range of turbulence length scales, which implies it is larger than the Kolmogorov scale η of viscous dissipation.

The instant velocity field can be split at any point of the flow as $\mathbf{u} = \overline{\mathbf{u}} + \mathbf{u}'$, where $\overline{\mathbf{u}}$ is the average velocity and $\mathbf{u}'$ is the turbulent fluctuation, the over bar symbol denoting the average over a large number of realizations.

Following the Hinze Kolmogorov theory which considers that the most efficient vortices for deformation are those of size comparable to that of the undeformed drop, the average turbulent force responsible for drop deformation is related to the average dynamic pressure difference between two points separated of a drop diameter distance, which scales as the second order structure function of velocity fluctuations at a distance d: $\overline{\delta u^2(x,d)} = \overline{\|\mathbf{u}'(x+d,t) - \mathbf{u}'(x,t)\|^2}$. From a Lagrangian point of view, if we consider $\overline{\delta u^2(d)}$ to be the averaged turbulent energy experienced by the drop along its path $x(t)$ in the turbulent field, the average turbulent stress at the drop scale is $F_{turb} = \rho_c \overline{\delta u^2(d)}$.

In a turbulent flow, successive and random interactions between vortices and the droplet cause oscillations of its shape; the dynamics of relaxation of the interface is then well described by the scales given previously which are the characteristic frequency of oscillation ω_2 and the damping rate β_2. Risso and Fabre[18] have shown in their experiment of a bubble in a homogeneous turbulent flow that the oscillation frequency ω_2 is dominant in the shape oscillation dynamics even in a turbulent flow, as illustrated in Figure 1. However, contrary to the drop dynamics, the turbulent flow does not contain a single characteristic frequency but a continuous spectrum of frequencies, each one being associated to a given power.

Nondimensional numbers and breakup conditions

Finally, the drop is characterized by a restoring force F_s and a frequency ω_2 and a rate β_2, whereas the flow exerts an average force intensity F_{turb} distributed over a broad range of frequencies. Another important time scale is the time of residence t_r of the drop in the flow, which is defined as the time spent by the drop in the turbulent field.

Based on these scales, a first analysis leads to the following nondimensional numbers that are relevant for the problem of drop deformation in a turbulent flow:

- the ratio between the time of residence of the drop and its oscillation period (which is its response time to shape perturbations): t_r/T_2;
- the average turbulent Weber number which compares the intensity of turbulent (pressure) fluctuations and the capillary force: $\overline{We} = \rho_c \overline{\delta u^2(d)}\, d/\sigma = F_{turb}/F_s$;
- the damping coefficient of the drop deformation dynamics, which compares the time scale of viscous damping to the period of shape oscillation: $\xi = \beta_2/\omega_2$.

Breakup is assumed to occur whenever either the Weber number or the amplitude of drop deformation exceeds a critical value. The first criterion is identical to the classical one that compares the deformation stress and the interfacial stress. Then, it disregards the response time of the drop, understating that the drop adjusts its deformation immediately after its

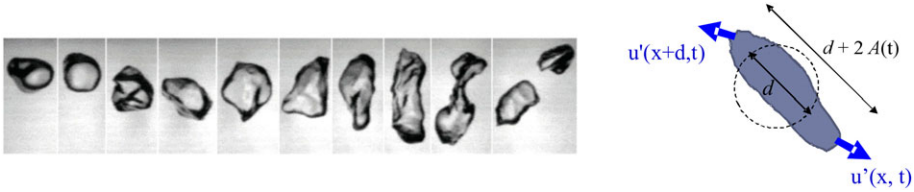

Figure 1. A bubble oscillating in a turbulent flow, and a scheme of a bubble deformed by turbulent fluctuations at its scale.

[Color figure can be viewed at wileyonlinelibrary.com]

interaction with an eddy. However, breakup can occur in zones of low averaged stress, as observed in Galinat et al.,[30] whereas it has been shown that droplets do systematically breakup above a given deformation; then, the alternative criterion of critical deformation is chosen here. In this study, we focus on the case of a two phase flow system with low to moderate viscosities, characterized by $\xi \ll 1$, where frequency and damping rate of drops or bubbles can be easily calculated from Eq. 1. Another important condition to be fulfilled is that surface tension is the main resistance force to deformation in the turbulent field. This criterion corresponds to small value of the Ohnesorge number based on the inner phase viscosity, defined as $Oh = \frac{\mu_d}{\sqrt{\rho_d \sigma d}}$ (note that $Oh = \frac{1}{Re_{OSC}} \frac{2\sqrt{3}}{\sqrt{\gamma}}$). Under this condition, experiments[30,31] show that the critical deformation corresponds to a drop elongation of about twice its initial diameter; in the case of a high internal viscosity (high Oh), much larger deformations can be reached,[31] so considering turbulent fluctuations at the initial drop size scale would not be sufficient for the prediction of breakup. Note that the condition $\xi \ll 1$ is not strictly equivalent to $Oh \ll 1$, and in the frame of the proposed model for breakup, both conditions have to be verified.

With the objective to compute an average drop breakup frequency, an important quantity to be scaled is the frequency of occurrence of eddies with a sufficient intensity. It must be noted that $\overline{We}$ can be the same for a flow with rare and strong vortices and a flow with moderate vortices appearing at a higher frequency. *A priori*, the information concerning the frequency of repetition of events of a given threshold is not contained in the turbulent spectrum. Consequently, a statistical study is required to characterize the breakup frequency and relate it to the relevant nondimensional parameters of the turbulent flow considered.

Drop breakup in homogeneous turbulence may result from two distinct mechanisms: (i) an interaction with a strong turbulent vortex, intense enough to provide a critical deformation, or (ii) a series of interactions with vortices of low or moderate intensity which make the droplet accumulating energy of deformation up to the critical deformation.

Mechanism (i) is the one considered in a critical Weber number We_{crit} approach because it corresponds to an instantaneous static balance of forces with a critical threshold as breakup criterion. This approach is relevant in case of a turbulence composed of rare eddies of sufficient intensity for breakup; in the latter case, statistics of occurrence of breakup events are similar to that of occurrence of intense eddies, as shown in the experimental device of Ravelet et al.[32] We could also think that a We_{crit} approach is able to predict breakup when the residence time of the drop in the turbulent field is negligible compared to the time scale of drop dynamics: $t_r \ll T_2$; however, such a static approach assumes an instantaneous breakup whereas a dynamic approach accounts for the finite response time of the drop to reach the critical deformation, hence statistics of breakup frequency are expected to be different between the two modeling approaches.

Mechanism (ii) of drop deformation due to a cumulative process can only be described by a dynamic approach. In this case, breakup results from the interaction between the drop and the repetition of eddies, each one with its own duration, which can be of moderate intensity (associated to a small Weber number). This resonance mechanism occurs when t_r is higher than T_2, and it is able to produce breakup events on long times. Note that, if the viscous damping of the oscillations is fast compared to the oscillating period $t_v \ll T_2$, this mechanism will not be effective in the deformation process; however, as we limit this study to droplets for which $\xi \ll 1$, this case is excluded here.

To conclude, the dynamic approach developed in this article is suitable whatever the time scales ratio and accounts for breakup mechanisms (i) and (ii). In the following, the oscillator model is presented and used in the limit of low ξ.

A model of forced oscillator for drop deformation and breakup

The model detailed here is the linear forced oscillator model first introduced in the article of Risso and Fabre.[18] It is a Lagrangian model that follows the interactions of the drop with the turbulent eddies along its trajectory. The model predicts the drop deformation in time, described through the amplitude of deformation $A(t)$ of Mode 2 which is assumed to be the first mode excited by turbulence. This amplitude represents the oscillation of the drop shape between a prolate (positive amplitude) and an oblate shape (negative amplitude), which is forced by the turbulent fluctuations at its scale; oscillations are driven by surface tension which is the restoring interfacial force in this model, and are damped by viscous effects either from the dispersed or the continuous phase.

This model simply relates the local turbulent fluctuations and the interface dynamics by means of a forced oscillator:

$$\frac{d^2A}{dt^2} + 2\beta_2 \frac{dA}{dt} + \omega_2^2 A = KF(t), \tag{2}$$

In this model Eq. 2, it is assumed that main vortices responsible for breakup are in average those of size comparable to that of the undeformed droplet, in accordance with the Kolmogorov theory. Then, $F(t)$ represents the forcing term due to the turbulent excitation at the drop initial scale d, which is written as $F(t) = \frac{\delta u^2(d,t)}{d}$, based on the instantaneous dynamic pressure difference experienced by the drop. ω_2 and β_2 correspond to the time scales of the response process of the drop shape. K scales the amount of kinetic stress which excites Mode 2. It is the only unknown parameter of this model that requires to be determined from experimental data.

This model predicts the drop deformation in time; because of the definition of the amplitude of Mode 2, the length associated to the maximal deformation writes $d + 2A(t)$ (cf Figure 1). It can be combined with a breakup critical value for $A(t)$.

By introducing the nondimensional numbers ξ and $We(t) = \rho_c \delta u^2(d, t) d/\sigma$, Eq. 2 can be written in its dimensionless form, with $\hat{a} = A/d$, $\hat{t} = t\omega_2$:

$$\frac{d^2\hat{a}}{d\hat{t}^2} + 2\xi \frac{d\hat{a}}{d\hat{t}} + \hat{a} = K' We(t), \tag{3}$$

in which $K' = K\sigma/\left(\rho_c d^3 \omega_2^2\right)$. Note that if K is constant, K' is also constant for a given $\hat{\rho}$ owed to the fact that ω_2 is close to the Lamb frequency ω_2^0.

The choice here is to consider the linear model of Eq. 3, with the use of ω_2 and β_2 calculated from a theory assuming small deformation around the spherical shape, and a description of turbulence and drop shape reduced each one to a unique scalar, as it is believed that this level of complexity is enough to capture the main mechanisms responsible for drop deformation when the drop viscosity is moderate (low ξ and

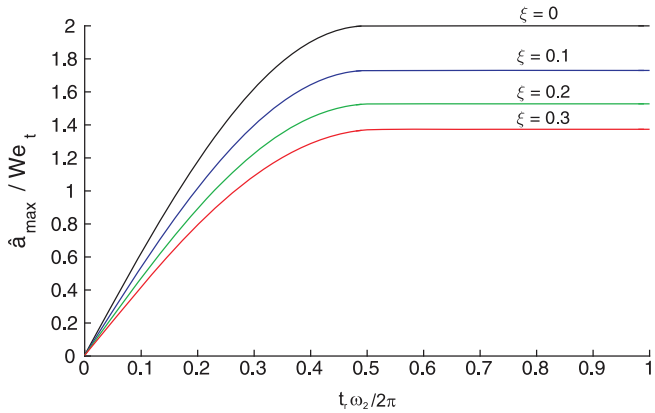

Figure 2. Maximal deformation $\hat{a}_{max}/We_t$ provoked by a single eddy of duration t_r and intensity We_t, at different ξ values.
[Color figure can be viewed at wileyonlinelibrary.com]

low *Oh*), in consistency with the theory of Kolmogorov Hinze for drop breakup in a turbulent flow.

Application of the model

In this section, the response of the dynamic model Eq. 3 is illustrated in some elementary cases.

Response to a Single Eddy. The first case corresponds to the interaction of a drop with an isolated eddy of intensity We_t during a time t_r. The forcing term in Eq. 3 is $We(t) = We_t$ when $0 \le t \le t_r$, and $We(t) = 0$ otherwise (with $K' = 1$). Solving this ODE allows to calculate the drop deformation, which is proportional to We_t; thus, we examine the normalized maximal deformation with time $\hat{a}_{max} = \max(\hat{a}(t))$, divided by We_t, which is plotted in Figure 2 as a function of the eddy duration t_r/T_2, and for different values of the damping coefficient ξ. Il is found that maximum deformation reaches its highest value when the eddy duration t_r is larger than $T_2/2$. In the inviscid case ($\xi = 0$), deformation is maximum and reaches $2We_t$. The higher ξ, the lower the drop deformation caused by the eddy.

Note also that the response time of the drop to reach the critical deformation $\hat{a}_{max}/We_t$ is always less or equal to $T_2/2$, depending on t_r; this corresponds to the finite time of deformation accounted for in this oscillator model.

Response to a Succession of Turbulent Eddies. The second case corresponds to the deformation of the drop by two consecutive eddies of same intensity We_t and duration $t_1 = T_2/2$, these two eddies being separated in time by Δt. The forcing term is $We(t) = We_t$ when $0 \le t \le t_1$ or $t_1 + \Delta t \le t \le 2t_1 + \Delta t$, and $We(t) = 0$ otherwise (with $K' = 1$).

After being deformed by the first eddy, the deformation can be cumulative depending on the instant the second eddy interacts with the drop: Figure 3 shows the cases of $\Delta t = T_2$, $T_2 + 1/4T_2$, $T_2 + 1/2T_2$, and $T_2 + 3/4T_2$. If the second eddy interaction occurs exactly after one (or an integer number of) oscillating period T_2, the drop deformation totally vanishes. However, in the other cases considered here, the deformation of the drop increases, the most efficient case corresponding to a second eddy occurrence at $T_2/2$. Then, it is concluded that the drop response after being deformed by two consecutive eddies depends both on their duration and their time spacing; there are cases where the drop deformation vanishes or is enhanced by the second eddy.

The third case corresponds to the interaction of the drop with periodic eddies of same intensity. We choose a duration of $T_2/2$ for each eddy of intensity We_t, which are separated by a time interval $\Delta_t = T_2/2$ to maximize deformation. Figure 4 shows the amplitude of deformation of the drop with time, for different values of $\xi = 0$, 0.1, 0.3. The cumulative process is the most efficient in the inviscid case. For $\xi > 0$, the maximal deformation increases during the first periods then saturates at a given value, which is a decreasing function of ξ. This graph illustrates how viscosity, either of internal or external phase (involved in the expression of β_2) resists to drop deformation.

A real turbulent flow is obviously not as simple as these examples. The different eddies seen by the drop along its

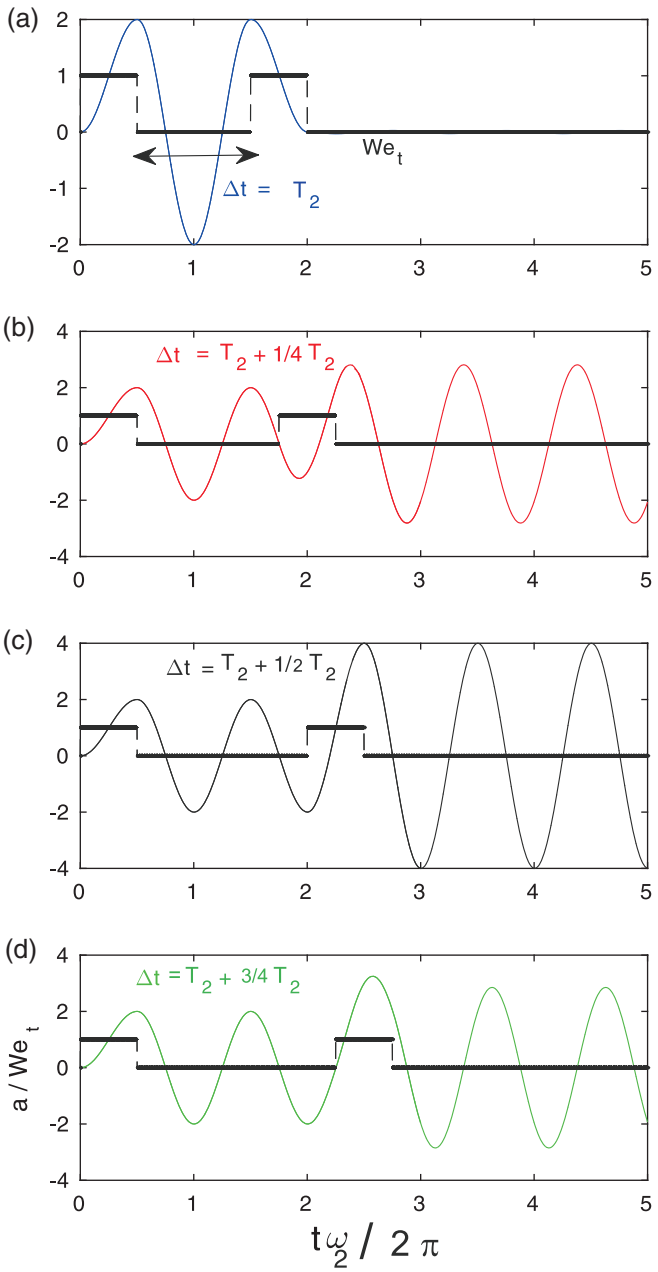

Figure 3. Amplitude of deformation of a drop deformed by two successive eddies: the first one of duration $T_2/2$ and the second one of same duration but after a time Δt, equal to (a) T_2, (b) $T_2 + 0.25T_2$, (c) $T_2 + 0.5T_2$, and (d) $T_2 + 0.75T_2$.
In any cases, $\xi = 0$. [Color figure can be viewed at wileyonlinelibrary.com]

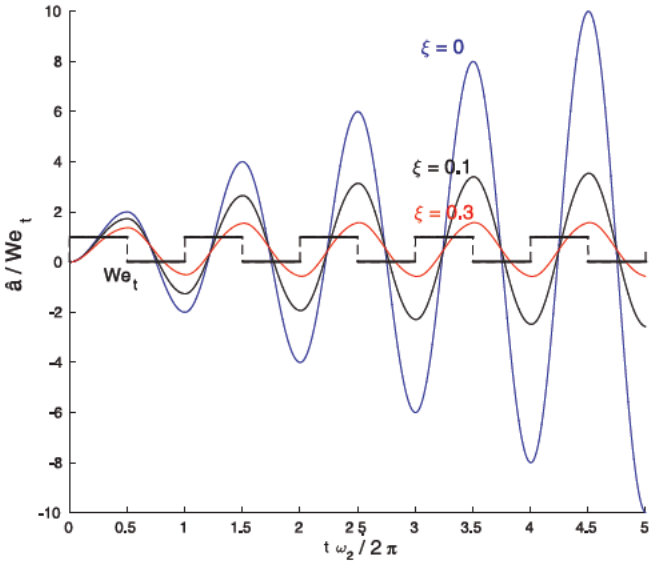

Figure 4. Amplitude of deformation of a drop deformed by five successive eddies of duration $T_2/2$ and separated in time with $T_2/2$, for ξ = 0, 0.1, 0.3.
[Color figure can be viewed at wileyonlinelibrary.com]

trajectory are of random intensity, random duration, and random frequency of occurrence.

The next section considers the case of deformation of a drop in a real turbulent flow, using an experimental forcing signal *We*(*t*).

Drop deformation in a turbulent flow and breakup statistics

The dynamic model of Eq. 3 has already been compared to experimental data of the breakup probability: in the case of bubbles in the paper of Risso and Fabre,[18] and in the case of droplets immersed in another liquid in the papers of Galinat et al.[19] and Maniero et al.[20] with an inhomogeneous turbulent flow. In this section, we evaluate the model of Eq. 3 on a new set of experimental data on breakup statistics of individual butyle benzoate droplets in an isotropic turbulent water flow.

An Experiment with Isotropic Turbulent Flow. The experiment consists of a drop released in a turbulent field generated by means of an axisymmetric turbulent jet discharged into a closed tube, the flow being described in detail in Risso and Fabre.[33] In the tube, the turbulence which is produced is inhomogeneous at large scale as all moments of the velocity decrease with the axial position but, in the central part where breakup is investigated, velocity fluctuations are nearly isotropic and homogeneous at the drop scale. In this way, the velocity temporal spectrum measured by laser Doppler anemometry in a point located in the observation window displays the classical −5/3 power law; at this point, intensity of turbulent fluctuations in the axial direction is $\sqrt{u'^2}$=0.99 m/s, while the mean flow velocity is $\overline{u}$ = 0.049 m/s, which corresponds to a kinetic energy of turbulence 12 times larger than that of the mean flow. At the center of the measurement region, the integral length scale is 20 mm, the Taylor length scale is 2 mm and the Kolmogorov microscale is η = 0.1 mm. Drops of butyle benzoate with a diameter between 1.1 and 10 mm are injected in the water flow; the physical properties of the liquid system are the following: ρ_c = 1000 kg/m^3, ρ_d = 1005 kg/m^3, μ_c = 0.001 Pa.s, μ_d = 0.0038 Pa.s, and σ = 0.02 N/m. The two phases having almost equal densities, the drift velocity of the drops is always negligible compared to $\sqrt{u'^2}$, ensuring that turbulence is the main cause of drop deformation and breakup in this flow.

The instantaneous turbulent forcing seen by a drop is given by the function of instantaneous velocity increments $\delta u^2(d, t) = [u'(z(t)) - u'(z(t) + d)]^2$. The temporal evolution of this quantity is not obtained directly from measurements but is estimated as follows. It is first assumed that the ratio between the instantaneous increment velocity function and the square of the velocity fluctuations is equal to the ratio of corresponding averaged values, that is, $\delta u^2(d,t)/u'^2(t) \approx \overline{\delta u^2(d)}/\overline{u'^2}$ (note that this assumption, also used in Ref. [18], would deserve to be validated by means of direct numerical simulations in a homogeneous and isotropic turbulent flow). Then, assuming local flow homogeneity in the vicinity of the measurement point, the second order structure function can be written as $\overline{\delta u^2(d)} = 2\overline{u'^2}[1 - B_{zz}(d)]$, where $B_{zz}(d) = \frac{\overline{u'(z)u'(z+d)}}{(\overline{u'^2(z)u'^2(z+d)})^{1/2}}$ is the velocity autocorrelation coefficient in z direction. Finally, we express the increment velocity function by

$$\delta u^2(d,t) = u'^2(t) \times 2[1 - B_{zz}(d)] \tag{4}$$

In this experiment, $B_{zz}(d)$ has been obtained from simultaneous measurements in two points and it has been shown that $\delta u^2(d, t) = u'^2(t) \times 2.51(d/D)^{2/3}$, D = 7.7 cm being the pipe diameter (cf Risso and Fabre[18]). Using this equation, the turbulent forcing $\delta u^2(d, t)$ experienced by a drop is computed from the instantaneous velocity signal u'.

Model for Drop Deformation. Figures 5 and 6 represent a sample of the experimental forcing signal K' *We*(*t*) (with K' = 1) and the corresponding deformation response signal $\hat{a}(t)$ for two

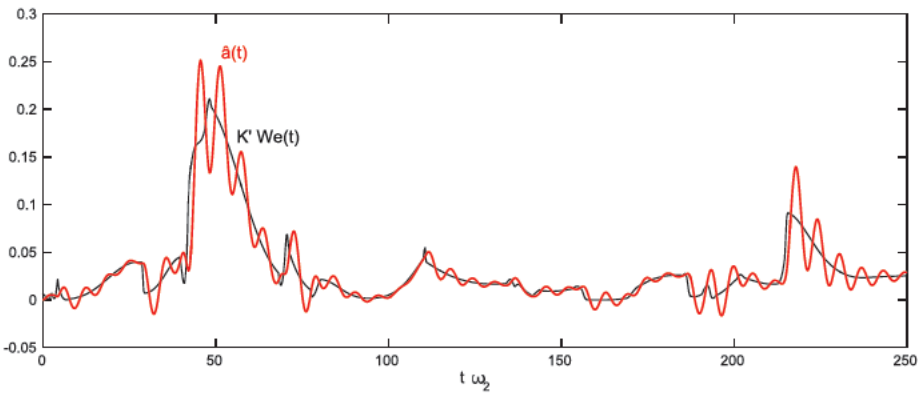

Figure 5. Response in deformation $\hat{a}(t)$ of a 2 mm drop to a turbulent forcing signal K' *We*(*t*).
[Color figure can be viewed at wileyonlinelibrary.com]

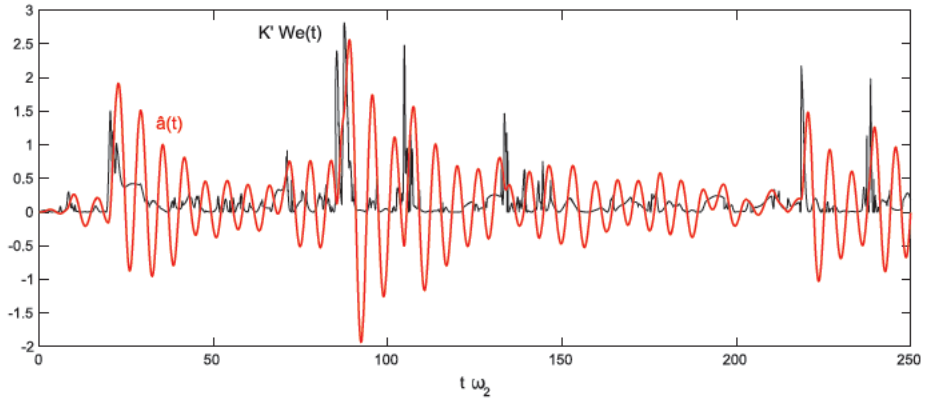

Figure 6. Response in deformation $\hat{a}(t)$ of a 10 mm drop to a turbulent forcing signal K' $We(t)$.
[Color figure can be viewed at wileyonlinelibrary.com]

drops of $d = 2$ mm and 10 mm, respectively, predicted from the resolution of Eq. 3. The frequency of occurence of eddies of given strength (i.e., given Weber number) is higher for the drop of 10 mm. For the smaller drop, the turbulent forcing can be considered as a low frequency forcing compared to ω_2, and the amplitude of deformation oscillates around the turbulent forcing; thus, the curve $K'We(t)$ also represents the shape deformation fluctuating signal. However, this is a regime where breakup is scarce because of the low intensity of the forcing. At the opposite, for the larger drop, the turbulent signal is a high frequency forcing, and it is observed that the drop filters out the turbulent fluctuations at its own time scale T_2 in such a way that some eddies favor drop deformation, whereas other ones are ineffective in deforming the drop or may help it to recover its spherical shape, depending on both eddy duration and occurence during the shape oscillation cycle. Consequently, two eddies of comparable intensity may not produce the same deformation, and there is no clear correlation between the occurence of an eddy of sufficient intensity and a breakup event contrary to what assumes a We_{crit} breakup criterion.

Breakup Probability. We compare here experimental statistics on breakup with the predictions of model Eq.3, by assuming a breakup criterion based on either a critical Weber number or a critical deformation (in the oscillator model). The breakup probability is defined as the relative number of broken drops among the initial population. In the experiments, statistics of breakup have been obtained from a population of 72 drops ranging between 2 mm and 10 mm (average diameter of 6.1 mm). Breakup events have been recorded in a finite size test section of the flow corresponding to well characterized turbulence statistics. In this study, the average turbulent Weber number lies in the range $0.1 \le \overline{We} \le 3.2$. In the oscillator model, 7200 drops have been same simulated with the same size distribution as in the experiments, using, in Eq. 4, the instantaneous experimental forcing (velocity) signal recorded in the test section as $u'(t)$. With the oscillator model, breakup is considered to occur when the drop deformation exceeds a critical value set to $\hat{a}_{crit} = 1$ that corresponds to a total length of $3d$ (because of a critical drop elongation of $2d$). This model has been computed with $K' = 0.4$. To compute breakup statistics, note that the value of $\hat{a}_{crit}$ is not of primary importance in the oscillator model as the actual adjustable parameter is the ratio $\hat{a}_{crit}/K'$ (set to 2.5 here). In contrast, with a critical Weber model, breakup is assumed to occur when the instantaneous Weber number reaches We_{crit} set also to 2.5 here, so only the knowledge of the forcing term in time is required with this breakup criterion.

Figure 7 compares the time evolution of the breakup probability of the experiment and computed from the oscillator model. It is concluded that the model is able to accurately predict the evolution of the breakup probability. In this particular case and in contrast with cases presented in Galinat et al.[19] and Maniero et al.,[20] the critical deformation and Weber number approaches give comparable results of the breakup probability. This is due to the fact that the drop size distribution considered in this experiment is mainly composed of drops between 4 and 8 mm whereas the deviation between the two approaches is observed to be larger for the smallest ($d \le 3$ mm) and the largest drops ($d \ge 9$ mm).

The present comparisons with experimental data constitute a new confirmation that the forced oscillator model of Eq. 3 is able to predict breakup statistics of either a drop or a bubble, provided that (i) the turbulent forcing experienced by the drop is known (either measured or calculated by DNS) and (ii) the time scales of the shape oscillations (given by Eq. 1) are known. This approach includes more physics than that contained in a critical Weber number model, as it accounts for the finite time of drop

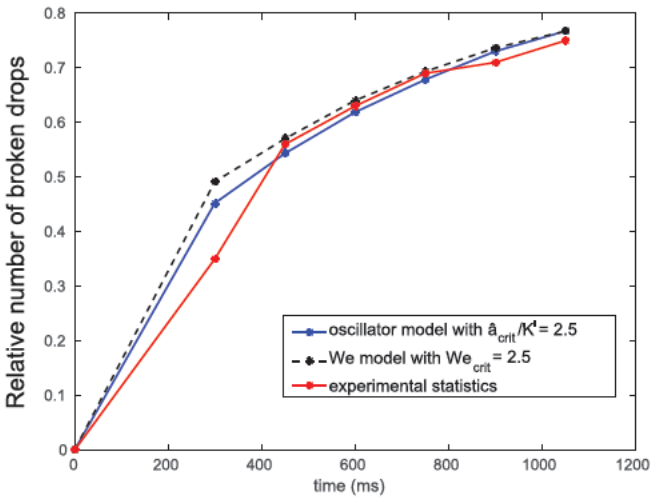

Figure 7. Time evolution of breakup probability (relative number of broken drops between $t = 0$ and a current time t) of drops in an isotropic turbulent flow: comparison between the experiment, the oscillator model Eq. 3 with $\hat{a}_{crit}/K' = 2.5$, and the critical Weber model with $We_{crit} = 2.5$.
[Color figure can be viewed at wileyonlinelibrary.com]

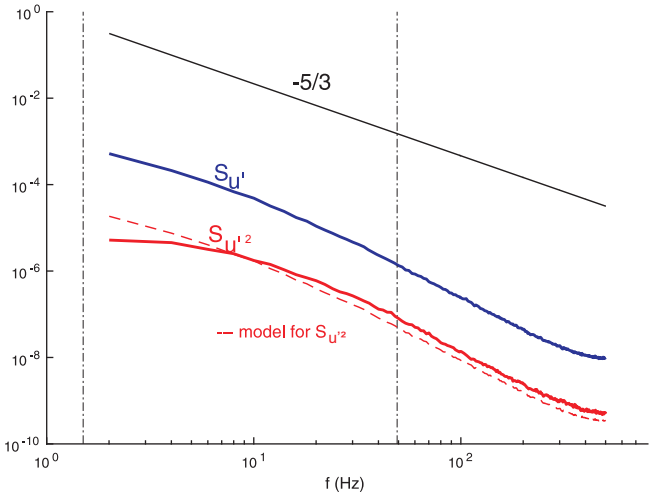

Figure 8. Power spectral density of the axial velocity fluctuations $S_{u'}(f)$ (unit: [m²/s]) and of their square $S_{u'^2}(f)$ (unit: [m⁴/s³]) measured inside the test section of the experiment considered in this article.

The two vertical lines correspond to the drop eigenfrequency f_2 of the largest and the smallest diameter (respectively, the smallest and the largest frequency). The model ( ) for $S_{u'^2}(f)$ corresponds to the computation of Eq. 12. [Color figure can be viewed at wileyonlinelibrary.com]

deformation, and is able to include both mechanisms of breakup (induced by a strong eddy or by resonance).

In the following, this dynamic model is used to compute statistics on the breakup frequency.

Breakup Frequency Model

In this section, the average breakup frequency of drops of different sizes is determined in the isotropic turbulent flow corresponding to the experiment described in the previous section. All the results presented here are obtained from the forced oscillator model, with again $\hat{a}_{crit}/K' = 2.5$. Then, an original model for the breakup frequency is proposed as a function of Eulerian statistical quantities of the flow and the damping coefficient of the oscillator, to include the effect of density and viscosity of both phases.

Statistics on the breakup frequency

Monodispersed populations of oil drops are considered, with diameters ranging from 2 to 20 mm, for which physical properties are those given in the previous section, except viscosity which is varied (either in dispersed or continuous phase) so as to investigate different values of ξ. In particular, the reference case is the inviscid one ($\xi = 0$), then ξ is changed by increasing the continuous phase viscosity up to a factor of 30, its maximal value being $\xi = 0.3$ (giving a maximal value of Oh of 0.18).

In this range of drop sizes, $0.2 \le \overline{We} \le 7.7$. The temporal spectrum of turbulent fluctuations $S_{u'}(f)$ of the continuous phase at the measurement point is displayed in Figure 8, where S denotes the power spectral density of the signal and f the frequency. The lowest and the highest eigenfrequencies of the drops ($f_2 = 2\pi/\omega_2$) are also indicated in this figure. The velocity spectrum is close to a $-5/3$ power law and the drop size lies within the inertial range of the turbulent spectrum.

For each drop size, the oscillator model of Eq. 3 is computed using the experimental forcing term corresponding to Eq. 4, this forcing being sampled at a frequency of 1 ms. Simulations are run until the drop reaches the breakup criterion. This numerical experiment is thus equivalent to droplets remaining in an isotropic and homogeneous turbulent field in a box, with infinite time of residence. For each drop size, the breakup frequency f_b is defined as the inverse of the average time that the drops remain in the flow before breaking up. In this simulation, the number of drops is large enough to obtain converged results both of the mean value and the standard deviation of the breakup time distribution.

For the inviscid cases ($\xi = 0$), Figure 9a displays the evolution of the breakup frequency as a function of the drop diameter, using the two approaches based on $\hat{a}_{crit}$ and $We_{crit} = \hat{a}_{crit}/K'$. f_b varies over one order of magnitude, from very low values (compared to the oscillating frequency f_2) for the smaller drops to higher frequencies for the larger ones for which f_b become of same order as f_2. As shown by the plot, breakup frequency is found to be an increasing function of diameter. However, the critical Weber number and the critical deformation approaches exhibit different trends, highlighting the contribution of the history of droplet deformation in the breakup process, even though the predictions of these two approaches are close in the range $5 \le d \le 10$ mm for the present system. As illustrated in Figure 9b, which shows the effect of ξ on the normalized breakup frequency f_b/f_2 obtained with the critical deformation criterion, increasing the damping coefficient tends to decrease f_b due to both a decrease of amplitude (same eddy intensity induces a smaller deformation) and a reduction of the possible cumulative process of deformation (mechanism of resonance). Finally, f_b depends on the turbulent intensity, on the repetition of strong enough vortices in the flow, and on the value of ξ.

Eulerian model for breakup frequency

The objective is to relate the values of f_b, obtained with the critical deformation criterion, to statistical characteristics of the turbulent fluctuations at the drop scale.

Time Evolution of the Variance of Deformation. Among the mathematical properties of a forced oscillator, when the forcing term is a stochastic process with a continuous spectrum, the time evolution of the variance $\overline{\dot{a}_2^2}$ of the oscillator estimated for a large number of realizations can be derived analytically under the assumption that the dominant contribution of the forcing term to oscillator amplitude is reached at the neighborhood of the resonance frequency of the oscillator (see Preumont[34]). This is equivalent to consider the forcing signal as a white noise, that is, a signal with a power spectral density independent of the frequency, taking the value of the spectral density at the oscillator resonance frequency. Note that, in the case of low ξ, the resonance frequency is nearly equivalent to the drop eigenfrequency ω_2. Then, the dynamics of the variance of the deformation depends on two parameters:

- the dimensionless power spectral density of the forcing term noted $\hat{S}_{K'We}$ and evaluated at the frequency of response of the oscillator, which represents the amount of energy of the forcing available at this frequency,
- the damping coefficient ξ.

This requires the knowledge of the power spectral density of the turbulent forcing $\hat{S}_{K'We}(\hat{f})$ at $\hat{f} = 1/(2\pi)$ to be known (this dimensionless function is evaluated at $1/(2\pi)$ because $\hat{f}$ is

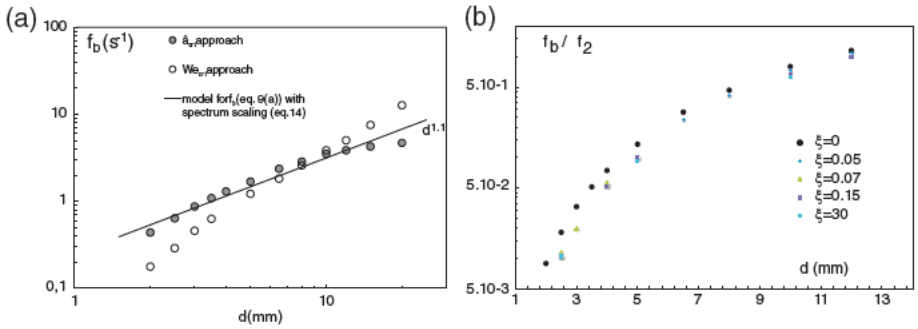

Figure 9. (a) Case $\xi = 0$—Breakup frequency f_b (1/s) as a function of the drop diameter d (mm): f_b is defined in the simulations as the inverse of the average time required to reach the breakup criterion for 30,000 droplets of each size. Points: experimental values for f_b obtained with a We_{crit} criterion ($We_{crit} = 2.5$) and a $\hat{a}_{crit}$ criterion (oscillator model with $\hat{a}_{crit} = 1$ and $K' = 0.4$). Line: prediction by model Eq. 9 combined with the scaling Eq. 14 of $\hat{S}_0 = \hat{S}_{K'We}(1/(2\pi))$. (b) Normalized breakup frequency f_b/f_2 for cases with different ξ, based on a $\hat{a}_{crit}$ criterion.

[Color figure can be viewed at wileyonlinelibrary.com]

scaled by the drop angular frequency ω_2); hereinafter, we define $\hat{S}_0 = \hat{S}_{K'We}(1/(2\pi))$.

The time evolution of the variance of deformation reads:

- in the inviscid case ($\xi = 0$):

$$\overline{\hat{a}_2^2} = \pi \hat{S}_0 \, \hat{t} \tag{5}$$

- in general case ($\xi > 0$):

$$\overline{\hat{a}_2^2} = \frac{\pi}{2\xi} \hat{S}_0 \left(1 - \exp^{-2\xi \hat{t}}\right) \tag{6}$$

The time evolution of the variance of drop deformation has been computed from statistics performed by considering 30,000 different samples of the turbulent signal. In Figure 10, results are compared with theoretical predictions given by Eqs. 5 and 6. A very good agreement is observed, showing that the variance of drop deformation linearly increases with time when $\xi = 0$. When $\xi > 0$, the variance linearly increases at short times, then saturates toward a constant value which is a decreasing function of ξ. The initial slope is nearly unaltered by ξ, due to the very slight sensitivity of the eigenfrequency to the phases viscosities (see Eq. 1).

Regarding the statistics of second order moment of drop deformation, these comparisons validate the approximation that the drop only responds to the amount of turbulent energy available at its eigenfrequency f_2 and filters out all the rest of the turbulent spectrum.

The power spectral density of the forcing of the oscillator at its resonance frequency describes the variance dynamics at short times. This value is not directly obtained from the classical temporal spectrum of fluctuation velocity u', but is related to the temporal spectrum of the increment velocity function $\delta u^2(d)$ seen by the drop over time. The dimensionless coefficient $\hat{S}_{K'We}(1/(2\pi))$ can be determined from Eq. 7 once evaluated the dimensional temporal spectrum of $\delta u^2(d)$ at the frequency f_2:

$$\hat{S}_0 = K'^2 \omega_2 \frac{\rho_c^2 d^2}{\sigma^2} S_{\delta u^2(d)}(f_2) \tag{7}$$

By making use of Eq. 4 to derive the power spectrum density of $\delta u^2(d)$ from that of u'^2, the value $\hat{S}_0$ of interest is then given by:

$$\hat{S}_0 = 4(1 - B_{zz}(d))^2 \, K'^2 \omega_2 \frac{\rho_c^2 d^2}{\sigma^2} S_{u'^2}(f_2) \tag{8}$$

In the discussion section, scaling laws will be proposed to determine $S_{u'^2}(f)$ from the usual temporal spectrum of u' denoted $S_{u'}(f)$.

Breakup Frequency Model. The time evolution of the deformation variance is well characterized by its growth rate, given by its initial slope $\pi \hat{S}_0$, and its saturation value, equal to $\frac{\pi}{2\xi}\hat{S}_0$. These nondimensional parameters could consequently also be relevant to predict the breakup frequency f_b, which is associated to a threshold of deformation. Nevertheless, this threshold corresponds to a critical instantaneous deformation, and the average time required to reach it for a set of drops of a given size is not directly given by the time necessary to get a threshold of the instantaneous deformation variance: at the instant corresponding to the average time of breakup f_b^{-1}, the deformation variance can be either still in its rising stage (for the largest drops with high f_b) or can already be converged at its saturation value (for the smallest drops with low f_b).

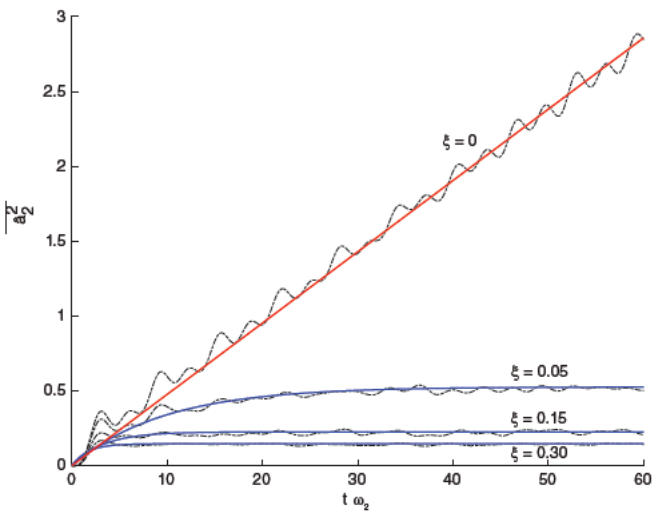

Figure 10. Variance of the amplitude of deformation $\overline{\hat{a}_2^2}$ as a function of time (d = 10 mm): comparison between numerical results (statistical averaging on 30,000 drops) [–. – .], and models: Eq. 5 for $\xi = 0$ and Eq. 6 for $\xi > 0$ (continuous lines).

[Color figure can be viewed at wileyonlinelibrary.com]

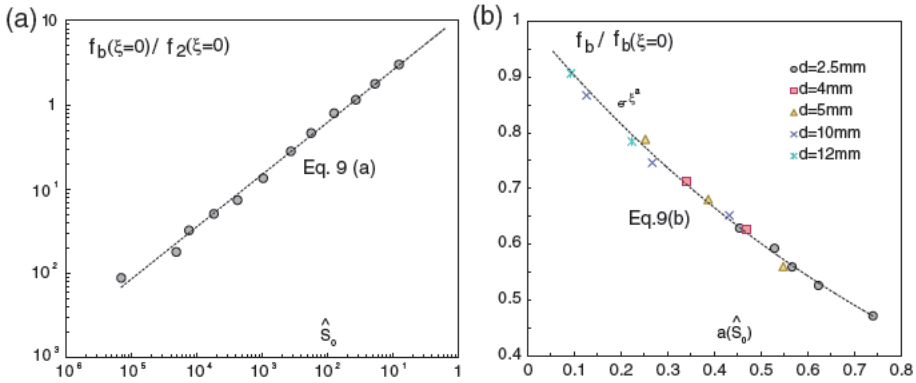

Figure 11. (a) Cases at $\xi = 0$: dimensionless breakup frequency f_b/f_2 as a function of the dimensionless power spectral density taken at the drop frequency $\hat{S}_0$. The dashed line corresponds to model of Eq. 9a in the case $\xi = 0$. (b) Viscous cases, with $0 < \xi \leq 0.3$: evolution of f_b, normalized by its value in the inviscid case, as a function of ξ^a, where a is a function of the reference value of $\hat{S}_0$. The dashed line corresponds to model of Eq. 9b in the case $\xi \leq 0.3$.

[Color figure can be viewed at wileyonlinelibrary.com]

However, in the inviscid case, Figure 11a shows that the breakup frequency normalized by the drop eigenfrequency is related to the dynamics of the deformation variance as it perfectly matches a power law of $\hat{S}_0$ (with an exponent close to 2/3), in the whole range of f_b/f_2 considered. The amount of energy of the forcing at the resonance frequency of the drop is thus a relevant parameter to characterize the breakup frequency at $\xi = 0$.

For the viscous cases ($0 < \xi \leq 0.3$), a correction can be introduced by analyzing the evolution of f_b compared to the inviscid case. In Figure 11b, we observe that the breakup frequency decrease can reach up to 50% of the value of f_b for $\xi = 0$, and, as expected, its rate of variation appears to be a growing function of $\hat{S}_0$. Then, it is found that the ratio between f_b at $\xi > 0$ and f_b at $\xi = 0$ can be well fitted by a decaying exponential law of ξ^a, where a is a slightly increasing power law of the value of $\hat{S}_0$, as plotted in Figure 11b.

Finally, provided that $\xi \leq 0.3$, the following correlation for the breakup frequency is obtained:

$$\frac{f_b(\xi=0)}{f_2(\xi=0)} = 10.74\ \hat{S}_0^{0.62} \tag{9a}$$

$$\frac{f_b}{f_b(\xi=0)} = \left[1-\xi^a+\frac{\xi^{2a}}{2}\right] \text{with} \, a = 1.53\ \hat{S}_0^{0.18}. \tag{9b}$$

Note that the eigenfrequency of the drop in the inviscid case has been used in the previous expressions: $f_2(\xi=0) = \frac{1}{2\pi}\sqrt{\frac{\sigma}{d^3}\frac{192}{(2\rho_c+3\rho_d)}}$.

Discussion on the model proposed for breakup frequency

The above Eulerian model (Eq. 9) of the breakup frequency requires the knowledge of two parameters $\hat{S}_0$ and ξ. This model accurately reproduces the values of f_b that have been computed from numerical experiments using a criterion of critical deformation at breakup $\hat{a}_{crit} = 1$ (with $K' = 0.4$). In the following, the sensitivity of f_b to the value of $\hat{a}_{crit}$ is discussed. Then, a scaling law for $\hat{S}_0$ in the inertial range of turbulence is proposed.

Influence of $\hat{a}_{crit}$ on f_b. In the context of this study with drops of relatively low viscosity, breakup is experimentally observed for moderate elongations of drops or bubbles. We consider here a range of critical amplitude of deformation $0.5 \leq \hat{a}_{crit} \leq 2$, that is, a critical maximum drop length between $2d$ and $5d$. Based on numerical experiments of breakup, the influence of $\hat{a}_{crit}$ on f_b in evaluated in Figure 12. The model of deformation Eq. 3 being linear, increasing the critical amplitude is equivalent to decrease constant K' of the forcing term. In this range of $\hat{a}_{crit}$, f_b can be considered as being proportional to $\hat{a}_{crit}$ with a good level of approximation, in the whole range of values of ξ and $\hat{S}_0$ investigated. As a consequence, the influence of $\hat{a}_{crit}$ can be simply implemented by changing Eq. 9a to:

$$f_b(\xi=0) = 10.74\ \hat{a}_{crit}\, f_2(\xi=0)\ \hat{S}_0^{0.62} \tag{10}$$

Scaling of $\hat{S}_0$ in the Inertial Range. The breakup frequency has been related to the value of $\hat{S}_0$, which can be

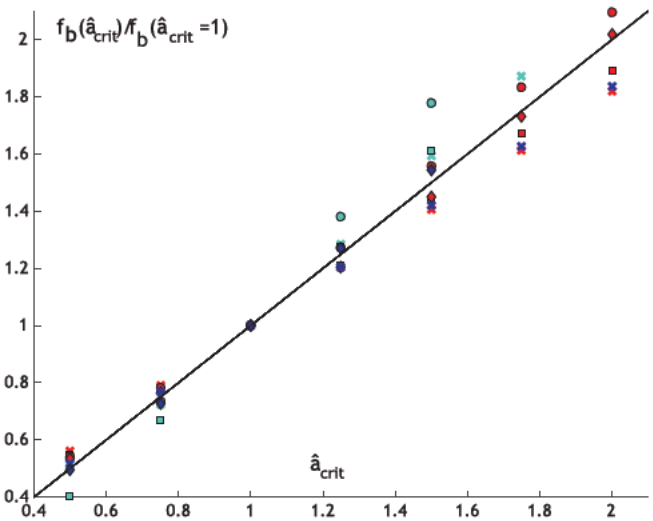

Figure 12. Sensitivity of measure of f_b to $\hat{a}_{crit}$ (by setting $K' = 0.4$): for drops of $d = 2.5$ mm (cyan color), $d = 5$ mm (blue color), $d = 10$ mm (red color), measure of f_b at different $\hat{a}_{crit}$ between 0.5 and 2, f_b being normalized by the breakup frequency of reference at $\hat{a}_{crit} = 1$.

Legend: crosses ($\xi = 0$), squares ($\xi \leq 0.1$), diamonds ($0.1 < \xi \leq 0.15$), and circles ($0.15 < \xi \leq 0.30$). [Color figure can be viewed at wileyonlinelibrary.com]

derived from the temporal spectrum of turbulent kinetic energy $S_{u'^2}(f)$ based on Eq. 8. Assuming a homogeneous and isotropic turbulence (HIT), this quantity can be scaled as a function of classical power spectrum of velocity fluctuations $S_{u'}(f)$.

In the inertial range of turbulence, the one dimensional temporal power spectrum of the velocity fluctuations, $S_{u'}(f)$, is a power law in $f^{-5/3}$ and writes:

$$S_{u'}(f) = \alpha\ (\sqrt{\overline{u'^2}})^{2/3}\ \epsilon^{2/3}\ f^{-5/3}, \tag{11}$$

where $\alpha = \frac{9}{55} C_k$, $C_k \approx 1.6$ is the Kolmogorov constant, $\overline{u'^2}$ is the variance of velocity fluctuations, and ϵ is the dissipation rate of the turbulent kinetic energy.

Introducing the time scale $T = \frac{\overline{u'^2}}{\epsilon}$ in Eq. 11, the normalized spectrum reads: $S_{u'}(f)\overline{u'^2} = \alpha\ T^{-2/3}\ f^{-5/3}$.

The power spectrum of kinetic energy $S_{u'^2}$ has been computed from the experimental signal and plotted in Figure 8. The curve exhibits the same power law as a function of frequency as the velocity power spectrum $S_{u'}$. Therefore, the normalized power spectrum (scaled by the fourth order moment of velocity fluctuations) is expected to scale like that of velocity power spectrum, leading to: $S_{u'^2}(f)\overline{u'^4} = \alpha\ T^{-2/3}\ f^{-5/3}$. This scaling law has also been verified by generating numerical velocity signals (with random phases in the complex plane), power spectrum of which follows a −5/3 power decay. Therefore, $S_{u'^2}(f)$ can be related to $S_{u'}(f)$ by:

$$S_{u'^2}(f) = S_{u'}(f)\frac{\overline{u'^4}}{\overline{u'^2}} \tag{12}$$

The accuracy of Eq. 12 to estimate $S_{u'^2}$ is illustrated in Figure 8. Note that the ratio $\overline{u'^4}/\overline{u'^2}$ is known as the product of the variance of velocity fluctuations by the flatness coefficient. Assuming the probability density function of the velocity fluctuations to be Gaussian, this ratio is equal to $3\overline{u'^2}$.

Hence, under the assumption of HIT, the power spectral density of the turbulent forcing taken at the inviscid drop eigenfrequency $f_2(\xi = 0)$ can be computed in the inertial range as a function of common turbulent statistical quantities, combining Eqs. 8, 12, and 11, leading to:

$$\hat{S}_0 = 24\pi\ \alpha\ (1 - B_{zz}(d))^2\ K'^2 \frac{\rho_c^2 d^2}{\sigma^2}\ \overline{u'^2}^{4/3} [f_2(\xi = 0)]^{-2/3}\ \epsilon^{2/3} \tag{13}$$

Making use of Eq. 4, the autocorrelation coefficient $B_{zz}(d)$ can be expressed as a function of the second order structure function $\overline{\delta u^2(d)}$ by $B_{zz}(d) = 1 - \frac{\overline{\delta u^2(d)}}{2\overline{u'^2}}$. In HIT, this quantity scales as $\overline{\delta u^2(d)} = \beta\ \epsilon^{2/3}\ d^{2/3}$ with $\beta = 4.82 C_k \approx 7.7$, following Batchelor.[35]

By combining these expressions with Eq. 13, the following scaling law for $\hat{S}_0$ in HIT is proposed:

$$\hat{S}_0 = \frac{3}{8\pi^3}\alpha\ \beta^2\ K^2 \left[\frac{\epsilon}{\overline{u'^2}\ f_2(\xi = 0)}\right]^2 \left[\frac{\overline{u'^2}}{(d\ f_2(\xi = 0))^2}\right]^{4/3} \tag{14}$$

To summarize, the implementation of Eq. 14 into Eqs. 9a and 9b gives a prediction of the breakup frequency as a function of Eulerian statistical quantities (ϵ and $\overline{u'^2}$) in the inertial range of a HIT flow, which provides a new breakup kernel for practical use in population balance equations provided these turbulent quantities are computed or measured. By combining these two equations and by applying this model on the experimental data previously presented, Figure 9a shows that the latter model predicts that f_b evolves as a power law of diameter $d^{1.1}$ (with all other physical parameters remaining constant), which is close to the evolution measured in the simulations.

An important remark is that this predictive model can be applied in heterogeneous turbulent flows, provided that the local values of ϵ and $\overline{u'^2}$ are known.

Finally, note also that the modeling approach which is proposed here is not limited to a particular form of the structure function $\delta u^2(d)$ and that other scalings of $\hat{S}_0$ could be obtained by integrating other structure functions in the development detailed in this article.

Discussion on the comparison with experimental breakup frequencies

Evaluation of the present breakup frequency law, Eq. 9, on other experimental sets (as those presented in Solsvik et al.[3]) is not a simple task as such a validation requires details which are not always specified in the related papers. Indeed, the knowledge of the local flow hydrodynamics at the scale of the drop is often missing and cannot be reduced to a global value of the dissipation rate, the flows being generally heterogeneous.

Moreover, the breakup frequency data are generally not resulting from a direct measurement but are considered to be the product of a breakup probability divided by a breaking time, which is not the definition used here and that may strongly impact the prediction of breakup statistics. A strong requirement for a relevant comparison using the present model is that breakup frequencies should be measured under the assumption of a sufficiently large residence time. Indeed, in the present work, we have obtained (and then correlated) f_b as the converged averaged breakup frequency value of breaking droplets, that is, having a breakup probability equal to 1 when residence time is infinite. Figure 13 presents the normalized probability density function of the breakup times of droplets of d = 5 mm and d = 10 mm, and the average value of these distributions: it shows that when the droplets are small (i.e., at low $\overline{We}$), t_r has to be sufficiently large to capture rare breakup events which can radically change the average value of the distribution which decays very slowly at long times. Here, droplets of d = 2.5 mm required a residence time

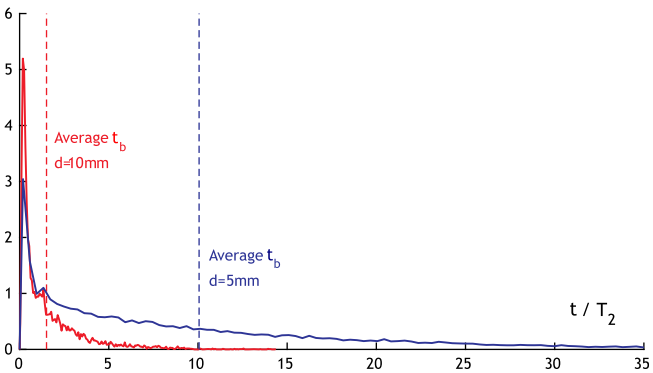

Figure 13. PDFs of the breakup times in the simulations (on 30,000 droplets) which give converged values of both the average breakup time $t_b = 1/f_b$ and its standard deviation, for diameters d = 5 mm and d = 10 mm (with ξ = 0.15).
[Color figure can be viewed at wileyonlinelibrary.com]

corresponding to 700 periods T_2 of oscillation, whereas it was of only $10T_2$ in the case of $d = 10$ mm.

In the experimental data of Wilkinson et al.[36] with air bubbles in a turbulent flow through a venturi shaped pipe, the residence time lies between $4T_2$ and $14T_2$ for all bubbles, which means that the experimental data do not fulfill the condition of sufficiently high residence time as the breakup probability is <0.6. The study of Martinez Bazan et al.[14] has been carried out in conditions where bubbles have very short residence times (t_r inferior to T_2), the same remark being valid with that of Eastwood et al.[13] with viscous droplets for which $t_r \approx T_2$. Finally, data of Maaβ and Kraume[37] correspond to breakup probabilities lying between 0.2 and 0.8; then, using either the maximal value of the peak of the distribution of breakup times or the average value of the latter distribution, they obtain opposite evolutions of f_b with the droplet diameter.

These two problems of convergence of breakup statistics and knowledge of local flow hydrodynamics in experiments make difficult any validation of the present breakup model from available experimental results, as it requires that data are obtained at the same scale level, and are converged in both space and time.

More generally, for validation purposes of the physical concepts used to derive any breakup model, relevant hydrodynamics conditions could be an HIT, at least in a local region of the flow.

Conclusion

In this study, the development of a new drop/bubble breakup frequency model in a turbulent flow has been proposed, which is valid in the case where turbulent pressure fluctuations of the carrier flow are responsible for breakup, and the resistance to deformation is controlled by the interfacial force (Ohnesorge number $Oh \ll 1$, that is, low damping coefficient ξ). Under these conditions, a dynamic model considers that the droplet or the bubble behaves as an oscillator of eigen frequency f_2, which is forced by the turbulent fluctuations at the drop scale. This case is relevant for many chemical engineering applications involving bubbles or droplet emulsions of moderate viscosity in a turbulent carrier phase. It turns to consider breakup events occurring for drop or bubble deformation of the order of their initial diameter. The novelty provided by the present approach is that the viscosities of both phases, as well as their densities, are explicitly included in the calculation of the drop oscillation characteristic times (the eigenfrequency f_2 and damping rate β_2) without resorting to any adjustable parameter, and showing that their roles are not symmetrical.

Based on this dynamic model of deformation, the breakup frequency f_b of droplets has been measured using experimental turbulent velocity signals. In this numerical experiment, time of residence t_r of the drops is infinite, allowing the computation of breakup frequency in a wide range of variation from $f_b/f_2 \ll 1$ (smallest drops) to $f_b/f_2 = O(1)$ (largest drops). f_b is found to be an increasing function of d, and viscous effects decrease f_b compared to the inviscid case, taken as reference.

Compared to classical approaches based on a We_{crit} for breakup, this dynamic model includes the mechanism of deformation resulting from the interaction of the drop with successive eddies leading to an increase of deformation by resonance. It is found that taking into account this mechanism leads a different power law of the breakup frequency as function of the drop diameter.

An important result of this study is the approach used for proposing an Eulerian model for f_b, from statistics performed on Lagrangian forced oscillators. This scale change has been possible thanks to the use of relevant nondimensional parameters. The choice of these parameters is based on the mathematical properties of the time evolution of the variance of a forced oscillator, that depends on (i) the power spectral density of the forcing taken at the resonance frequency of the oscillator $\hat{S}_0$ and (ii) the damping coefficient ξ of the oscillator. Hence, it has been possible to propose a model, Eq. 9, for the breakup frequency that relies only on these two parameters. This model is valid provided that $\xi \leq 0.3$ and residence time is large enough ($t_r \gg T_2$). For application purposes, $\hat{S}_0$ has been related in Eq. 14 to local statistical properties of a turbulent flow (dissipation rate and variance of velocity fluctuations, that can be computed by Eulerian CFD codes), using scaling laws valid in the inertial range of a homogeneous and isotropic turbulent flow.

In practical applications with emulsions, which often involve excess of surfactants and saturated interfaces or multilayers, the interface stress tensor cannot be reduced to a constant interfacial tension, as adsorbed surfactants are susceptible to form networks at the interfaces with visco elastic properties. Note that this case is beyond the scope of this article, and is generally not addressed in other literature devoted to the development of breakup kernels in chemical engineering applications. However, the present dynamic model could be extended by including such complex interfacial rheology effects (Gibbs and intrinsic surface elasticity, dilatation and shear surface viscosity) on the drop characteristic times f_2 and β_2, thanks to the theoretical framework of Miller and Scriven[24] or Lu and Apfel[25] on drop shape oscillation, which is another strength of such an oscillator model for the droplet.

Concerning breakup in turbulent emulsification processes, in the case of highly viscous droplets in such a way that $Oh > 1$, the drop deformation becomes controlled by the internal viscosity that tends to stretch the droplet in long filaments. Then, interfacial forces (such as surface tension) can be disregarded and the present oscillator model is not able to describe the droplet deformation statistics in time. This problem constitutes another interesting although rather complex regime to investigate,[38,39] due to the quite important number of related industrial applications.

Notation and Greek letters

R undeformed radius, m
d undeformed diameter, m
Re_{OSC} Reynolds number of oscillation: $Re_{OSC} \quad \frac{\rho_d \omega_2^0 d^2}{4\mu_d}$
We Weber number $We \quad \frac{\rho_c \delta u^2(d,t) d}{\sigma}$
Oh Ohnesorge number $Oh \quad \frac{\mu_d}{\sqrt{\rho_d \sigma d}}$
f_2 frequency of Mode 2 of oscillation $f_2 \quad 2\pi/\omega_2$, 1/s
T_2 period of Mode 2 of oscillation: $T_2 \quad 2\pi/\omega_2$, s
t_v viscous time of damping of Mode 2 of oscillation: $t_v \quad 1/\beta_2$, s
$f_2(\xi \quad 0)$ inviscid frequency of Mode 2 of oscillation $f_2(\xi \quad 0) \quad 2\pi/\omega_2^0$, 1/s
$\overline{u}$ time averaged value of the velocity component u, m/s
u' velocity fluctuation around the averaged value, m/s
A amplitude of oscillation (of Mode 2), m
t_r time of residence, s
$\hat{a}$ nondimensional amplitude of oscillation (of Mode 2) $\hat{a} \quad A/d$
$\hat{a}_{crit}$ critical nondimensional amplitude for breakup
We_t Weber number associated to a turbulent eddy
$F(t)$ dimensional instantaneous turbulent forcing at the drop scale $F(t) \quad \frac{\delta u^2(d,t)}{d}$, m/s^2
F_{turb} average turbulent stress at the drop scale $F_{turb} \quad \rho_c \overline{\delta u^2(d)}$, Pa
F_s interfacial stress that resists to deformation $F_s \quad \frac{\sigma}{d}$, Pa

$\hat{t}$ nondimensional time $\hat{t} \quad t\,\omega_2$
K constant of the deformation model
K' constant of the dimensionless deformation model $K' \quad K\sigma/(\rho_c d^3 \omega_2^2)$
$\overline{u'^2}$ variance of velocity fluctuations, m^2/s^2
$B_{zz}(d)$ longitudinal velocity correlation coefficient
$S_X(f)$ temporal spectrum of quantity X
C_k Kolmogorov constant $C_k \approx 1.6$
f_b breakup frequency, 1/s
$\widehat{f_2}$ nondimensional frequency of oscillation $\widehat{f_2} \quad 1/(2\pi)$
$\hat{S}_0$ nondimensional value of the temporal spectrum of K' *We* evaluated at the nondimensional resonance frequency: $\hat{S}_0 \quad \hat{S}_{K'We}(1/(2\pi))$
ρ_c density of the continuous phase, kg/m^3
ρ_d density of the dispersed phase, kg/m^3
$\hat{\rho}$ ratio of densities: $\hat{\rho} \quad \rho_c/\rho_d$
μ_c dynamic viscosity of the continuous phase, Pa.s
μ_d dynamic viscosity of the dispersed phase, Pa.s
$\hat{\mu}$ ratio of viscosities: $\hat{\mu} \quad \mu_c/\mu_d$
σ interfacial tension, N/m
ω_2 angular frequency of Mode 2 of oscillation, rad/s
ω_2^0 inviscid angular frequency of Mode 2 of oscillation: $\omega_2^0 \quad \sqrt{\frac{\sigma}{d^3}\,\frac{192}{2\rho_c + 3\rho_d}}$, rad/s
β_2 damping rate of Mode 2 of oscillation, 1/s
ξ nondimensional damping coefficient of the oscillator: $\xi \quad \beta_2/\omega_2$
η Kolmogorov scale in the turbulent flow, m
$\delta u^2(d, t)$ instantaneous structure function of Order 2 expressed at a separation distance equal to d, m^2/s^2
α constant: $\alpha \quad (9/55)\ C_k$
β constant $\beta \approx 7.7$
ϵ dissipation rate of a turbulent flow, m^2/s^3

Literature Cited

1. Lasheras JC, Eastwood C, Martinez Bazan C, Montanes JL. A review of statistical models for the breakup of an immiscible fluid immersed into a fully developed turbulent flow. *Int J Mult Flow*. 2002;28: 247 278.
2. Liao Y, Lucas D. A literature review of theoretical models for drop and bubble breakup in turbulent dispersions. *Chem Eng Sci*. 2009;15: 3389 3406.
3. Solsvik J, Tangen S, Jakobsen HA. On the constitutive equations for fluid particle breakage. *Rev Chem Eng*. 2013;29(5):241 356.
4. Kolmogorov AN. On the breakage of drops in a turbulent flow. *Dokl Akad Navk*. 1949;66:825 828.
5. Hinze JO. Fundamentals of the hydrodynamics mechanisms of splitting in dispersion process. *AIChE J*. 1955;1:289 295.
6. Coulaloglou CA, Tavlarides LL. Description of interaction processes in agitated liquid liquid dispersions. *Chem Eng Sci*. 1977;32:1289 1297.
7. Narsimhan G, Gupta JP. A model for transitional breakage probability of drops in agitated lean liquid liquid dispersions. *Chem Eng Sci*. 1979;34:257 265.
8. Lehr F, Millies M, Mewes D. Bubble size distributions and flow fields in bubble columns. *AIChE J*. 2002;48:2426 2443.
9. Wang T, Wang J, Jin Y. A novel theoretical breakup kernel function for bubbles/drops in a turbulent flow. *Chem Eng Sci*. 2003;58:4629 4637.
10. Prince MJ, Blanch HW. Bubble coalescence and breakup in air sparged bubble columns. *AIChE J*. 1990;36:1485 1499.
11. Tsouris C, Tavlarides LL. Breakage and coalescence models for drops in turbulent dispersions. *AIChE J*. 1994;40:395 406.
12. Luo H, Svendsen HF. Theoretical model for drop and bubble breakup in turbulent dispersions. *AIChE J*. 1996;42:1225 1233.
13. Eastwood CD, Armi L, Lasheras JC. The breakup of immiscible fluids in turbulent flows. *J Fluid Mech*. 2004;502:309 333.
14. Martinez Bazan C, Montanes JL, Lasheras JC. On the break up of an air bubble injected into a fully developed turbulent flow. Part I: break up frequency. *J Fluid Mech*. 1999;401:157 182.
15. Risso F. The mechanisms of deformation and breakup of drops and bubbles. *Multiphase Sci Technol*. 2000;12:1 50.
16. Sevik M, Park SH. The splitting of drops and bubbles by turbulent fluid flow. *J. Fluid Eng*. 1973;3:53 60.
17. Zhao H, Ge W. A theoretical bubble breakup model for slurry beds or three phase fluidized beds under high pressure. *Chem Eng Sci*. 2007; 62:109 115.
18. Risso F, Fabre J. Oscillations and breakup of a bubble immersed in a turbulent field. *J Fluid Mech*. 1998;372:323 355.
19. Galinat S, Risso F, Masbernat O, Guiraud P. Dynamics of drop breakup in inhomogeneous turbulence at various volume fractions. *J Fluid Mech*. 2007;578:85 94.
20. Maniero R, Masbernat O, Climent E, Risso F. Modeling and simulation of inertial drop break up in a turbulent pipe flow downstream of a restriction. *Int J Mult Flow*. 2012;42:1 8.
21. O'Rourke PJ, Amsden AA. The TAB method for numerical calculation of spray drop. *SAE Tech Paper*. 1987;218:872089.
22. Rayleigh JWS. On the capillary phenomena of jets. *Proc Royal Soc*. 1879;29:71 79.
23. Lamb H. *Hydrodynamics*. Cambridge University Press; 1932.
24. Miller CA, Scriven LE. The oscillations of a fluid drop immersed in another fluid. *J Fluid Mech*. 1968;32:417 435.
25. Lu HL, Apfel RE. Shape oscillations of drops in the presence of surfactants. *J Fluid Mech*. 1991;222:351 368.
26. Prosperetti A. Normal mode analysis for the oscillations of a viscous liquid drop in an immiscible liquid. *J Mec*. 1980;19:149 182.
27. Lalanne B, Tanguy S, Risso F. Effect of rising motion on the damped shape oscillations of drops and bubbles. *Phys Fluids*. 2013;25:112107.
28. Lalanne B, Abi Chebel N, Vejraka J, Tanguy S, Masbernat O, Risso F. Non linear shape oscillations of rising drops and bubbles: experiments and simulations. *Phys Fluids*. 2015;27:123305.
29. Abi Chebel N, Vejražka J, Masbernat O, Risso F. Shape oscillations of an oil drop rising in water: effect of surface contamination. *J Fluid Mech*. 2012;702:533 542.
30. Galinat S, Masbernat O, Guiraud P, Dalmazzone C, Nok C. Drop break up in turbulent pipe flow downstream of a restriction. *Chem Eng Sci*. 2005;60(23):6511 6528.
31. Andersson R, Andersson B. On the breakup of fluid particles in turbulent flows. *AIChE J*. 2006;52:2020 2030.
32. Ravelet F, Colin C, Risso F. On the dynamics and breakup of a bubble rising in a turbulent flow. *Phys Fluids*. 2011;23:103301.
33. Risso F, Fabre J. Diffusive turbulence in a confined jet experiment. *J Fluid Mech*. 1997;337:233 261.
34. Preumont A. 1990. Vibrations Aleatoires et Analyse Spectrale. *Presses Polytechniques Universitaires* Republished in English: Random Vibration and Spectral Analysis Kluwer; 1994.
35. Batchelor GK. *The Theory of Homogeneous Turbulence*. Cambridge University Press; 1956.
36. Wilkinson PM, Van Schayk A, Spronken JPM. The influence of gas density and liquid properties on bubble breakup. *Chem Eng Sci*. 1993; 48:1213 1226.
37. Maaβ S, Kraume M. Determination of breakage rates using single drop experiments. *Chem Eng Sci*. 2012;70:146 164.
38. Biferale L, Meneveau C, Verzicco R. Deformation statistics of sub Kolmogorov scale ellipsoidal neutrally buoyant drops in isotropic turbulence. *J Fluid Mech*. 2014;754:184 207.
39. Vankova N, Tcholakova S, Denkov ND, Ivanov IB, Vulchev VD, Danner T. Emulsification in turbulent flow: 1. Mean and maximum drop diameters in inertial and viscous regimes. *J Colloid Interface Sci*. 2007;312:363 380.